

*Climatic trends and different drought adaptive capacity and vulnerability in a mixed *Abies pinsapo*–*Pinus halepensis* forest*

Climatic Change

An Interdisciplinary,
International Journal Devoted
to the Description, Causes and
Implications of Climatic Change

ISSN 0165-0009

Volume 105
Combined 1-2

Climatic Change (2010)
105:67-90
DOI 10.1007/
s10584-010-9878-6

Climatic Change

An Interdisciplinary, International Journal Devoted to the
Description, Causes and Implications of Climatic Change

Editors: **MICHAEL OPPENHEIMER**
GARY YOHE

Volume 105 – Nos. 1–2 – March 2011



ISSN 0165-0009

 Springer

 Springer

Your article is protected by copyright and all rights are held exclusively by Springer Science+Business Media B.V.. This e-offprint is for personal use only and shall not be self-archived in electronic repositories. If you wish to self-archive your work, please use the accepted author's version for posting to your own website or your institution's repository. You may further deposit the accepted author's version on a funder's repository at a funder's request, provided it is not made publicly available until 12 months after publication.

Climatic trends and different drought adaptive capacity and vulnerability in a mixed *Abies pinsapo*–*Pinus halepensis* forest

Juan Carlos Linares · Antonio Delgado-Huertas ·
José Antonio Carreira

Received: 6 May 2009 / Accepted: 18 May 2010 / Published online: 17 June 2010
© Springer Science+Business Media B.V. 2010

Abstract The projected temperature rise, rainfall decrease and concentration of rainfall in extreme events could induce growth decline and die-off on tree populations located at the geographical distribution limit of the species. Understanding of adaptive capacity and regional vulnerability to climate change in Mediterranean forests is not well developed and requires more focused research efforts. We studied the relationships between spatiotemporal patterns of temperature and precipitation along the southwestern edge of the Betic range (southern Spain) and measured basal area increment (BAI) and carbon isotope (Δ) in tree ring series of *Abies pinsapo* and *Pinus halepensis*, two Mediterranean conifer trees with contrasting drought adaptive capacity. Climatic information was obtained from a network covering a wide range of elevations and distances from the Atlantic and Mediterranean coasts. Temperature trends were tested by the Mann–Kendall test, and precipitation was thoroughly analyzed by quantile regression. Climatic data showed a warming trend, enhanced since the 1970s, while quantile regressions revealed that drought events worsened

Electronic supplementary material The online version of this article (doi:10.1007/s10584-010-9878-6) contains supplementary material, which is available to authorized users.

J. C. Linares (✉)
Área de Ecología, Universidad Pablo de Olavide,
Ctra. Utrera km. 1, 41002, Sevilla, Spain
e-mail: jclincal@upo.es

A. Delgado-Huertas
Laboratorio de Biogeoquímica de Isótopos Estables,
Instituto Andaluz de Ciencias de la Tierra CSIC, Camino del Jueves s/n,
18100 Armilla, Granada, Spain
e-mail: antonio.delgado@eez.csic.es

J. A. Carreira
Área de Ecología, Universidad de Jaén,
Campus Las Lagunillas, 23071, Jaén, Spain
e-mail: jafuente@ujaen.es

during the course of the twentieth century. Long-term decrease of *A. pinsapo* BAI was related to regional warming and changing precipitation patterns, suggesting increasing drought stress on this species. Both temperature and precipitation in the summer influenced wood Δ in *P. halepensis*, whereas negative correlation between wood Δ and current autumn temperature was yielded for *A. pinsapo*. Increased intrinsic water use efficiency was inferred from wood Δ in both species; however, *A. pinsapo* showed sudden growth reductions under drier conditions, while pine trees were able to maintain almost constant BAI values and lower water costs under increasing long-term water stress.

1 Introduction

Climate observations prove the existence of a global warming trend which is expected to modify the growth and distribution of tree species. Trees are particularly sensitive to temperature changes (Adams et al. 2009); however forests vulnerability to climate change still contains large uncertainties (Lindner et al. 2010). Regional climatic models project both a warming and an extreme events enhancement over the Mediterranean basin at the end of the twenty-first century (Trigo and Palutikof 2001; Räisänen et al. 2004). The effects of these changes could be particularly severe in water-limited ecosystems (Martínez-Vilalta et al. 2008). The temperature trends have been widely verified. For instance, a warming of $0.042^{\circ}\text{C}/\text{year}$ has been reported for Europe since the 1970s (Klein Tank et al. 2002). In the western Mediterranean basin, the temperature trend shows an increase of about $0.053^{\circ}\text{C}/\text{year}$ for the same time span (Brunetti et al. 2004; Giorgi 2002; Brunet et al. 2005).

Overall, the precipitation trends in the Mediterranean basin during the last 50 years seem to be characterized by an increase in both the frequency and intensity of severe drought events (Piervitali et al. 1997; Türkes and Erlat 2003; Serra et al. 2005; García et al. 2007; Lana et al. 2008; Vicente-Serrano and Quadat-Prats 2007; Vicente-Serrano et al. 2004; Brunetti et al. 2004; Xoplaki et al. 2004). However, precipitation trend studies have shown uncertain results. Trends are generally not significant or significant only during some months and in some localities, without a clear spatial pattern (Norrant and Douguédroit 2006; Touchan et al. 2005; Chbouki et al. 1995; González-Hidalgo et al. 2001; Goodess-and-Jones 2002; Sumner et al. 2001; Esteban-Parra et al. 1998; Maheras and Anagnostopoulou 2003). The inherent rainfall variability observed in the Mediterranean region often prevents the detection of long-term trends using standard regression procedures, as standard errors of estimated parameters tend to be large and do not allow for the rejection of the null hypothesis of an absence of trend. This confounding effect appears to be even more important when long-term changes differ across the range of values taken by the variable of interest, a common feature of climatic changes. Here, as a first issue of the paper, we show how trends can be investigated in a specific range of the rainfall distribution by using quantile regression (Koenker 2005). We thus obtain a detailed picture of the patterns of climate change, when some of these patterns could have gone undetected using more traditional statistical analyses.

Recent papers propose tree growth vulnerability to climate change could be assessed as a function of the climate impacts and the trees' growth sensitivity and adaptive capacity (Lindner et al. 2010). Hence, climate effects on tree growth will

depend on the specific climate changes at regional scale, the inherent trees' species sensitivity and their ability to cope with the impacts (Allen et al. 2010; McDowell et al. 2010; Linares et al. 2010). While many studies have investigated potential impacts of climate change, much less attention has been given to the related tree growth sensitivity and adaptive capacity and few non theoretic researches have been focused under this conceptual framework to assess inter-specific vulnerability to climate change in the Mediterranean mountain conifer forests (but see Linares et al. 2009a and 2010). Among the dominant conifer species in the Mediterranean mountain forests, there are both drought-sensitive relict taxa and wide-spread drought-adapted trees (Médail and Quézel 1999). Different responses to increasing climate dryness could have important implications for the geographical range of trees in these ecosystems (Brubaker 1986). Pinsapo fir (*Abies pinsapo* Boiss.) and Aleppo pine (*Pinus halepensis* Mill.) are representative examples of both functional types of conifers. Although the two species can be considered as drought-avoiding, they show considerable differences in their ecophysiological response thresholds for coping with drought. *A. pinsapo* drastically reduces water use by stomatal closure in response to moderate drought conditions (Aussenac 2002), while *P. halepensis* is better adapted to the scarcity of water resources (Borghetti et al. 1998).

Both species currently grow in mixed stands at the lower elevation limit of some *A. pinsapo* forests, i.e., in the Yunquera forest (YF, Sierra de las Nieves Natural Park, southern Spain). This forest represents one of the drier and warmer locations of *A. pinsapo* habitats but is simultaneously one of the wetter localities in which *P. halepensis* grows (Linares et al. 2009a). In the study area, Pinsapo fir stands are usually found as dense monospecific stands at elevations above 1200 m, mainly on north-facing, shady slopes and ravine bottoms. On the other hand, Aleppo pine populations from YF grow naturally as open stands in shallow and stony soils on south- and east-facing slopes. Historical forestations have traditionally benefited the pine, and nowadays, its distribution reaches several peripheral margins of relict *A. pinsapo* stands (see [Supplementary material](#)).

Dendroecological studies combined with carbon isotope discrimination (Δ) in tree rings from these marginal stands could be valuable tools to assess the growth-climate relationships at the limit of the species distribution range (Andreu et al. 2007), where recent episodes of *A. pinsapo* decline related to climatic change have been described (Linares et al. 2009a). We hypothesized that contrasting ecophysiological thresholds in response to water deficits in *A. pinsapo* and *P. halepensis* would lead to a differential sensitivity and adaptation capacity to changes in water availability and that this could be tracked by means of radial growth and Δ analysis. To test this hypothesis, we compared the responses of the two species in terms of basal area increment (BAI) and wood Δ . We assumed that wood Δ would provide an integrated record of the intrinsic water use efficiency (WUE_i) during the growth period, whereas BAI would indicate the effect of water shortage on the overall tree functioning. The assessment of the ecological relevance of drought as a constraint on water and carbon ecophysiology could provide helpful information to forecast future responses of these species to climatic change (McDowell et al. 2010; Allen et al. 2010).

Our aims were: (1) to quantify regional precipitation and temperature trends over the twentieth century in the southwest of the Betic Range; (2) to simultaneously describe the recent annual radial growth and wood $\delta^{13}\text{C}$ patterns in *A. pinsapo* and

Pinus halepensis; and (3) to quantify BAI, Δ and WUEi responses to climate and the effects of different thresholds on drought sensitivity for two drought-avoiding conifer species.

2 Materials and methods

2.1 Climatic data

Data sets from 25 nearby meteorological stations were explored in order to select those with reliable data; then, 12 meteorological stations were selected based on their longest and best-quality series (Table 1, see also [Supplementary material](#)). For each station, missing data were estimated using the MET program from the Dendrochronology Program Library (Holmes 1992). The annual rainfall in year t was calculated as the sum of rainfall from September in year $t - 1$ to August in year t . Monthly variables were transformed into normalized standard deviations to give each station the same weight in calculating the average values for each month and year. The annual water budget was obtained as the sum of monthly differences between precipitation data and potential evapotranspiration estimates following a modified version of the Thornthwaite method (Willmott et al. 1985).

2.2 Field sampling

Field sampling was carried out at Yunquera forest (YF, southern Spain: 36°43'18.97" N, 4°57'53.92" W, 1,180–1,230 m a.s.l.), which is home to natural unevenly aged stands that have not been managed within the last 50 years (Linares and Carreira 2009). This location represents the lower elevation limit of *Abies pinsapo* at the Sierra de las Nieves Natural Park. Pinsapo forests are typically found above ~1,000 m a.s.l., below this, the vegetation is Mediterranean, dominated by *Quercus rotundifolia* Lam. (holm oak), *Quercus faginea* Lam. (gall oak) and *Pinus halepensis* Mill. (Alepo pine) forests. Upslope, *A. pinsapo* forms pure stands to roughly 1,700 m, where it grows with other relict trees, such as *Quercus faginea* subsp. *alpestris* (Boiss.) Maire, *Acer granatense* Boiss., *Sorbus aria* (L.) Crantz. and *Taxus baccata* L. The mean annual temperature is ~11°C, and the annual precipitation ranges from 1,100 mm to approximately 1,600 mm. As a whole, the rainfall patterns are distinctly Mediterranean, with approximately 80% of all precipitation falling between October and May, followed by a long summer drought. Since the studied stands have not been disturbed within the last 50 years, few dominant trees need to be sampled to obtain a reliable growth pattern related to the regional climatic signal (Fritts 1976). In winter 2006 we bored mature, dominant and healthy trees, sampling ten *A. pinsapo* and six *P. halepensis* trees, cored to the pith at breast height perpendicularly to the slope. Cores were 5 mm in diameter for both species. At least three cores per tree were extracted, and pith was reached in at least one of each set.

2.3 Dendrochronological methods

Dendroecological analysis was conducted for all cores for age determination and radial growth measurement. The cores were sanded until the tree rings were clearly

Table 1 Main characteristics of the meteorological stations included in the study (network: INM, Instituto Nacional de Meteorología; CHS: Confederación Hidrográfica del Sur)

Met Station	Location	Network	Span	Latitude (N)	Longitude (W)	Elevation (m)	Distance to the sampling site (km)	Distance to the coast (km)	Mean annual precipitation (mm)	Mean annual temperature (°C)
AZ	Alozaina	CHS	1929–2000	36°44'40"	4°51'20"	386	9.7	24.4	614	18.50
B	El Burgo	INM	1965–2003	36°56'47"	4°56'51"	580	7.6	33.3	595	15.23
C	Coín	INM	1947–2003	36°39'31"	4°45'37"	209	19.4	17.2	622	18.65
FP	Herriza	INM	1965–1999	37°08'05"	4°43'48"	425	49.5	54.1	456	16.96
GA	Gaucín	INM	1948–2003	36°31'06"	5°19'03"	626	44.5	16.8	1,107	15.40
GH	Guadalhorce	INM	1961–2003	36°56'47"	4°47'28"	325	29.0	42.7	500	16.53
GR	Grazalema	INM	1912–2003	36°45'32"	5°21'58"	823	36.0	41.9	2,015	15.31
P	Pilar de Tolox	CHS	1971–2006	36°41'18"	5°01'21"	1,715	6.2	22.3	1,585	
PR	Porrejón	CHS	1948–2003	36°30'37"	5°10'54"	1,056	10.3	34.2	1,270	
Q	Los Quejigales	INM	1965–2001	36°41'22"	5°02'47"	1,283	8.0	23.5	1,265	10.65
R	Ronda	CHS	1939–1987	36°44'31"	5°10'01"	700	18.0	33.3	627	
TB	Teba	INM	1965–2003	36°58'59"	4°55'17"	555	27.7	53.2	477	15.88

visible under a binocular microscope. All samples were visually cross-dated. Tree ring widths were measured to 0.01 mm using a LINTAB measuring device (Rinntech, Germany), and the cross-dating quality was checked using COFECHA (Holmes 1983). The trend of decreasing ring width with increasing tree size was removed by converting measurements of radial increment into tree BAI. Following the determination of BAI, a detrending and normalizing procedure was applied as follows. First, we calculated moving average BAI curves using 5-year windows; we chose this lag based on climatic and ecological research performed in the Mediterranean basin, which found that a 5-year lag was a reliable window to use to smooth high-frequency fluctuations and extreme events (Feidas et al. 2007; Sumner et al. 2001; Sarris et al. 2007). We subsequently calculated the BAI residuals, subtracting each value from the moving average. Since analyzing residuals in a subsequent statistical procedure, as we have done here, could result in misleadingly estimates of the significance, because the residuals themselves are based on estimates and have some inherent dependencies, we normalized the residuals to give each tree the same weight in calculating the average values for each year and used a non-parametric test. These normalized residuals enabled us to correlate deviations from the average growth (unrelated to any age effect) with climate throughout the overall study period (Schweingruber 1988).

2.4 Wood samples and isotopic analyses

Isotopic analyses were performed on six *A. pinsapo* and three *P. halepensis* trees selected from the entire sample. In order to minimize complications arising from the juvenile effect, which results in more negative values of $\delta^{13}\text{C}$ in wood produced during the first few decades of growth as a consequence of assimilating respired CO_2 depleted in ^{13}C or reduced light levels (Heaton 1999), we excluded the first 15–20 tree rings of each core. Then, annual tree rings were carefully separated with a razor blade supported by a binocular microscope and they were then ground in a ball mill (Retsch MM400, Germany). An aliquot of 0.5–0.7 mg of wood sample was weighed and placed in a tin capsule for isotopic analysis. The isotope ratio $^{13}\text{C}/^{12}\text{C}$ was determined on a Thermo Finnigan Delta plus XP mass spectrometer coupled to a Thermo Finnigan Trace GC ultra gas chromatographer by a Thermo Finnigan GC Combustión III interface. For every ten wood samples, we included two standards for analysis: cellulose, with an isotopic signal of -24.72 , and Ptalic acid, with an isotopic signal of -30.63 . The repeated analyses of these two internal standards yielded a standard deviation of less than 0.1%. Cellulose was not extracted, as whole wood and cellulose isotope time series show similar trends. The small tree ring size complicates further manipulation (Taylor et al. 2008; McNulty and Swank 1995; Warren et al. 2001).

2.5 Temporal trends of carbon discrimination and intrinsic water use efficiency

The isotopic discrimination (Δ ; Farquhar and Richards 1984) between carbon from atmospheric CO_2 and plant carbon from C_3 plants, which occurs as a result of preferential use of ^{12}C over ^{13}C during photosynthesis, is defined in Eq. 1:

$$\Delta = (\delta^{13}\text{C}_{\text{atm}} - \delta^{13}\text{C}_{\text{wood}}) / \left(1 + \delta^{13}\text{C}_{\text{wood}} / 1000\right), \quad (1)$$

where $\delta^{13}\text{C}_{\text{atm}}$ and $\delta^{13}\text{C}_{\text{wood}}$ are the isotopic ratios of carbon ($^{13}\text{C}/^{12}\text{C}$) in atmospheric CO_2 and plant material, respectively, expressed in parts per thousand (‰) relative to VPDB standard. Δ is linearly related to C_i/C_a , which is the ratio of intercellular (C_i) to atmospheric (C_a) CO_2 mole fractions, by Eq. 2 (Farquhar et al. 1982):

$$\Delta = a + (b - a) C_i / C_a, \quad (2)$$

where a is the fractionation during CO_2 diffusion through the stomata (4.4‰; O'Leary 1981), and b is the fractionation associated with reactions by Rubisco and PEP carboxylase (27‰; Farquhar and Richards 1984). C_a and $\delta^{13}\text{C}_{\text{atm}}$ were obtained from published data by McCarroll and Loader (2004).

The C_i/C_a ratio reflects the balance between net assimilation (A) and stomatal conductance for CO_2 (g_c) according to Fick's law: $A = g_c(C_a - C_i)$. Stomatal conductances for CO_2 and water vapor (g_w) are related by a constant factor ($g_w = 1.6g_c$), hence linking the leaf gas exchange of carbon and water. The linear relationship between C_i/C_a and Δ (Eq. 2) is often used to calculate the intrinsic water use efficiency, $\text{WUE}_i = A/g_w$:

$$\text{WUE}_i = c_a (b - \Delta_{\text{lin}}) / 1.6 (b - a). \quad (3)$$

The intrinsic water use efficiency, defined as the ratio of net assimilation of stomatal conductance to water vapor, was introduced to compare photosynthetic properties independent of (or with a common) evaporative demand (Osmond et al. 1980) and has been widely related to long-term trends in the internal regulation of carbon uptake and water loss in plants.

2.6 Statistical analyses

Temporal trends in tree ring width, $\delta^{13}\text{C}_{\text{wood}}$, Δ and WUE_i were tested by linear least squares regression, while mean values from different time intervals were subjected to analysis of variance (repeated measures ANOVA). We also applied a two-slope comparison test following Zar (1999) in order to detect rate differences among *A. pinsapo* and *P. halepensis*. Temporal trend of monthly mean temperature and monthly total precipitation were estimated using the Mann–Kendall test (Mann 1945; Kendall 1975).

Mann–Kendall tests (thereafter MK) are non-parametric tests for the detection of trend in a time series. These tests are widely used in environmental science, because they are simple, robust and can cope with missing values and values below a detection limit.

For each time series element x_i ($1, 2, \dots, n$), the number n_i of x_j elements lower than x_i ($x_j < x_i$, where $j < i$) are counted. Then, the MK statistic for the time series $\{Z_k, k = 1, 2, \dots, n\}$ is defined as:

$$T = \sum_{j < i} \text{sgn}(Z_i - Z_j) \quad (4)$$

where:

$$\text{sgn}(x) \begin{cases} 1, & \text{if } x > 0 \\ 0, & \text{if } x = 0 \\ -1, & \text{if } x < 0 \end{cases}$$

If no ties between the observations are present and no trend is present in the time series, the test statistic is asymptotically normal distributed with mean $E(t) = 0$, independent of the distribution function of the data. The statistic $E(T)$ is defined as:

$$E(T) = \frac{T - \langle T \rangle}{\sqrt{\text{Var}(T)}} \tag{5}$$

where $\langle T \rangle$ and $\text{var}(T)$ are computed as:

$$\langle T \rangle = \frac{n(n-1)}{4}$$

$$\text{var}(T) = \frac{n(n-1)(2n+5)}{18}$$

The null hypothesis assumes that the trend is zero and it is rejected if $E(T)$ is higher, in absolute value, than 1.96, for a two tails test at 95% significance, or 2.58 at 99% of significance. The $E(T)$ sign indicates if the trend is positive or negative. The MK test also allows to obtain a summarized trend of the data by the estimation of a multivariate analyses of the monthly data, which was interpreted in this paper as a summarized annual trend. When significant trends were obtained from MK tests, the rates of change of the climatic variables were estimated by obtaining their slope from simple linear regression (Libiseller and Grimvall 2002).

Quantile regressions were applied on the annual rainfall at each station, which allowed us to estimate the rate of change of any part of the data distribution, i.e., of any selected quantile, with the i th one-sample quantile estimate defined as the value having a proportion i of the sample observations less than or equal to the estimate (e.g., the median is the 0.5 quantile, and 50% of the observations are above its value and 50% are below its value). Therefore, quantile regression allows one to simultaneously study changes in specific portions of the distribution of the response variable, independent of the change and variability experienced by the rest of the distribution. In particular, its ability to detect opposing trends in statistical extremes (upper and lower) hidden in non-significant mean effects as well as changes in median conditions even in extreme stochastic environments makes it perfectly designed for climate analysis, although it has rarely been used in such a context (Koenker 2005; Cade and Noon 2003).

Correlations between monthly climate, BAI and Δ were tested by the non-parametric Spearman correlation r . As a first step, we investigated the correlations between the mean monthly temperature and precipitation of the three closest stations to the sampling area (Q, B and AZ, see Table 1) and BAI and Δ data. As a second step, regional climate relationships were investigated using the mean monthly temperature and precipitation of the remaining nine stations from Table 1; the initial

three stations were excluded to avoid autocorrelation with the initial correlation analysis (Table 1).

The significance level used in all tests was $P = 0.05$. Quantile regression analyses were conducted using the R *quantreg* package (R Development Core Team 2010). Mann–Kendall tests were performed using a free application download from http://www.etsm.slu.se/ShowPage.cfm?OrgenhetSida_ID=8144.

3 Results

3.1 Climatic trends

The studied climate data set allows us to recognize the influence of elevation and longitude (distance to the Atlantic Ocean) on temperature and precipitation (Table 1). The mean annual temperature decreased by an average of 0.72°C for every 100 m of elevation (the slope for linear regression \pm standard deviation was: -0.67 ± 0.11 ; R^2 adj. 0.87, $p < 0.001$), but was not correlated to either longitude or distance to the coast. The annual rainfall decreased towards the east by an average of 173 mm for every 10 km (172.50 ± 52.26 ; R^2 adj. 0.42, $p = 0.005$) and increased by an average of 81 mm for every 100 m of elevation (81.06 ± 20.95 ; R^2 adj. 0.50, $p = 0.002$). The distance to the coast did not show a significant correlation with annual rainfall. Temperature time series showed strong inter-site relationships, while the precipitation data were more locally variable. All studied localities showed a significant increase in temperature during some months, with March being the month with the most significant regional increase, followed by April, May and June (data not shown). The resulting regional monthly average temperature can be considered as highly representative of the regional trends; however averaged regional precipitation results must be carefully evaluated. Annual and seasonal analyses of mean temperature (Fig. 1, left column) show a warming of about 0.42°C since 1970 for the study area. All seasons except autumn and all months except September and October showed a significant temperature increase. This warming was markedly enhanced during February, March, June and July, with an increase of more than 0.56°C since 1970.

Annual P-ETP decreased significantly, with a reduction of -134 mm since 1970. Seasonal analyses did not show significant trends, and only the months of March and June showed a marginally significant decrease (Fig. 1, right column). However, the variability of rainfall data suggests that further analyses should be applied across the geographical area to obtain a reliable spatiotemporal precipitation pattern. There was no significant long-term trend in the mean (median) annual rainfall at ten of the 12 stations (the 0.5 quantile was only significant at GR and marginally at R, Fig. 2). However, such results mask important patterns in the rainfall changes. The quantile regression analyses revealed that the lowest part of the rainfall distribution, i.e., the driest years, experienced negative trends over the study period at eight of the 12 stations (Fig. 2). Furthermore, this rainfall decrease in the 0.1 quantile was spatially related to the distance to the coast (Table 1; see also [Supplementary material](#)). Thus, the localities nearest to the coast showed steady trends (PR, GA and C) that were independent of either the elevation (PR is at high, GA at middle and C at low

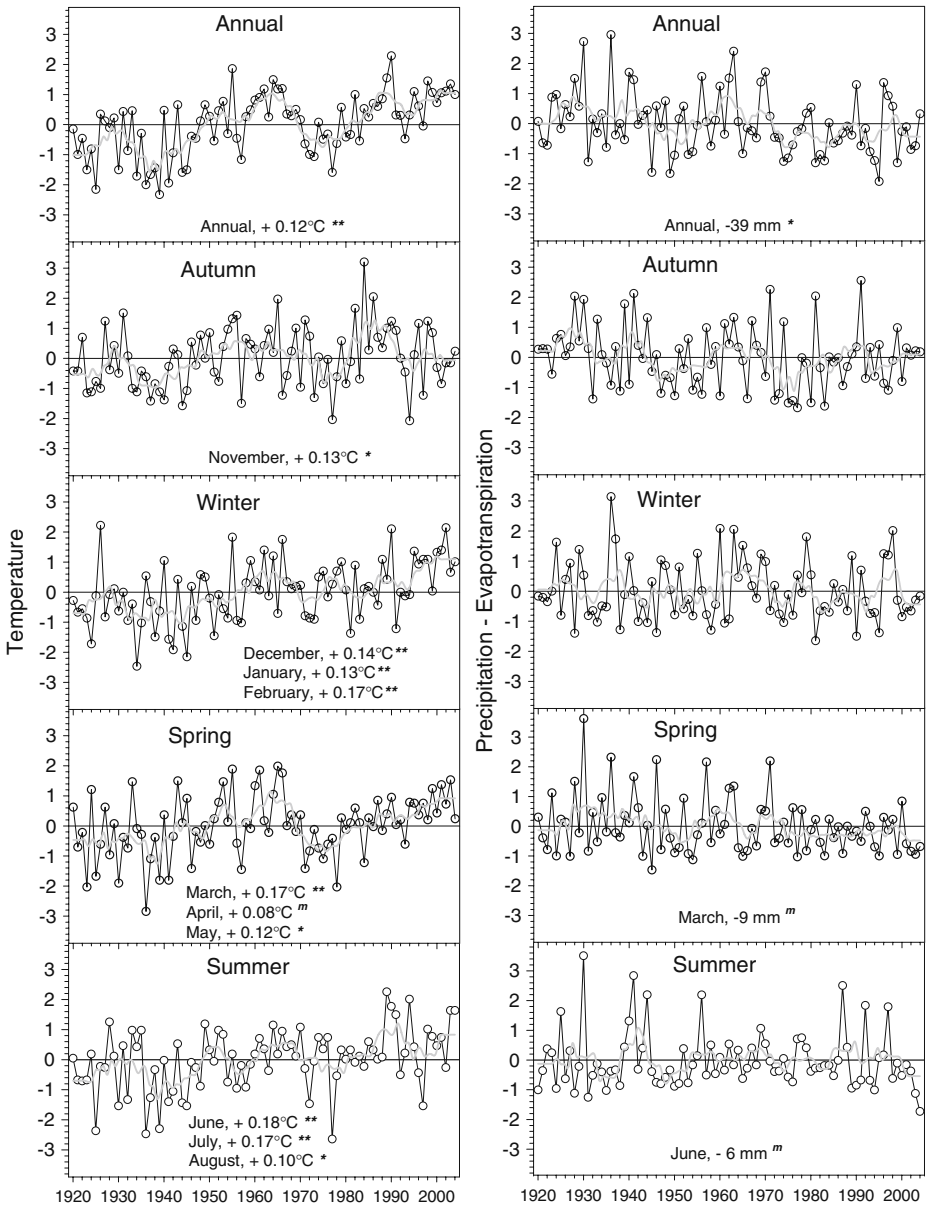


Fig. 1 Deviations from the available data mean in annual and seasonal mean temperature (*left column*) and precipitation minus evapotranspiration (*right column*). Months with significant trends and the average slope per decade are noted; significance denoted by *two asterisks* ($p < 0.01$), *one asterisk* ($p < 0.05$) and *m* ($p < 0.10$)

elevation) or the latitude (PR and GA are in the west, and C is in the east; see Table 1). In contrast, the stations most remote from the coast (i.e. FP, TB, GH, B and GR) showed more strongly decreasing rates in the lower quantile regression

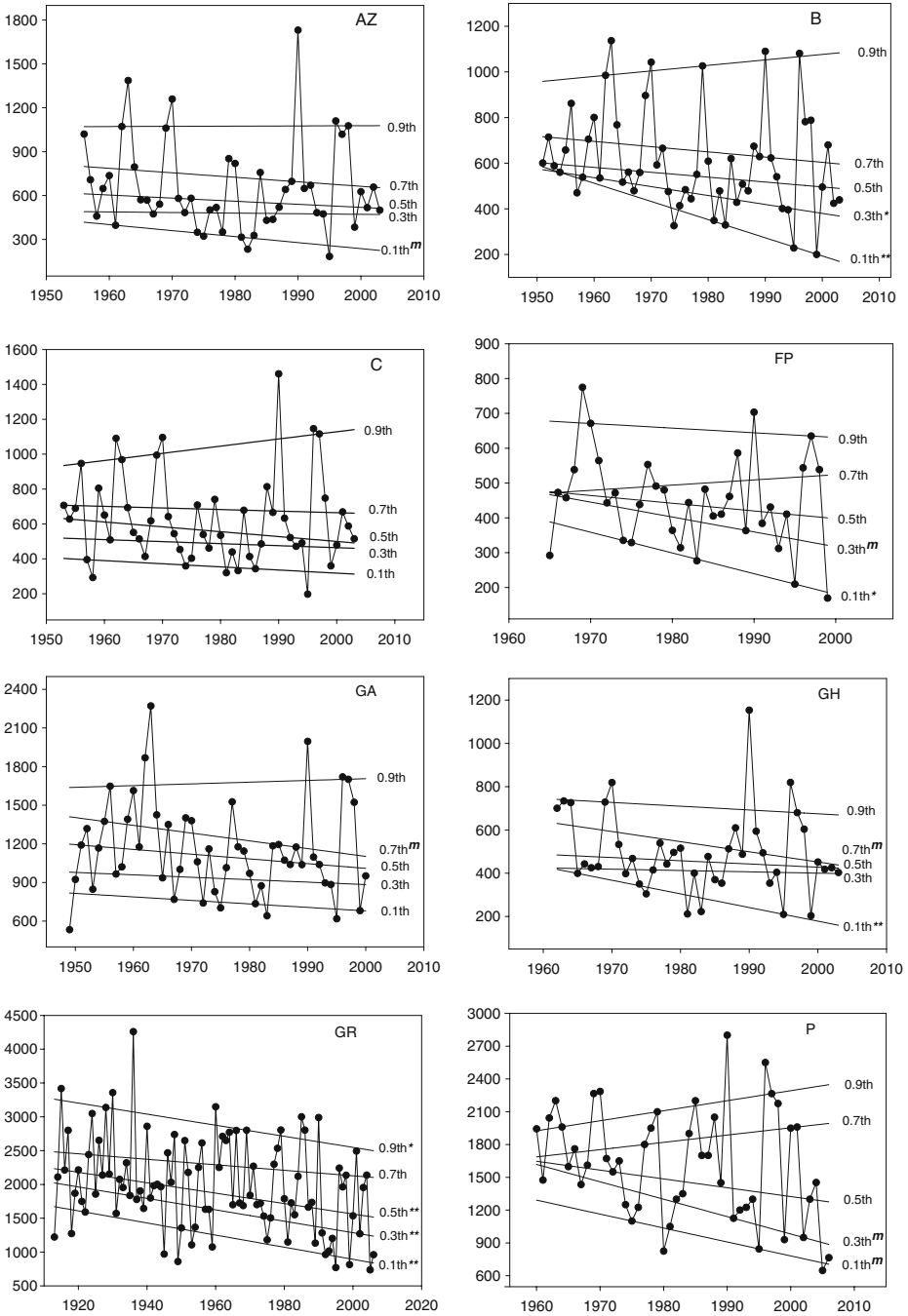


Fig. 2 Annual rainfall (points) for the 12 selected stations (see also Table 1). Solid lines show the 0.1, 0.3, 0.5, 0.7 and 0.9 quantile regression fits. Significant trends are noted as two asterisks ($p < 0.01$), one asterisk ($p < 0.05$) and m ($p < 0.10$)

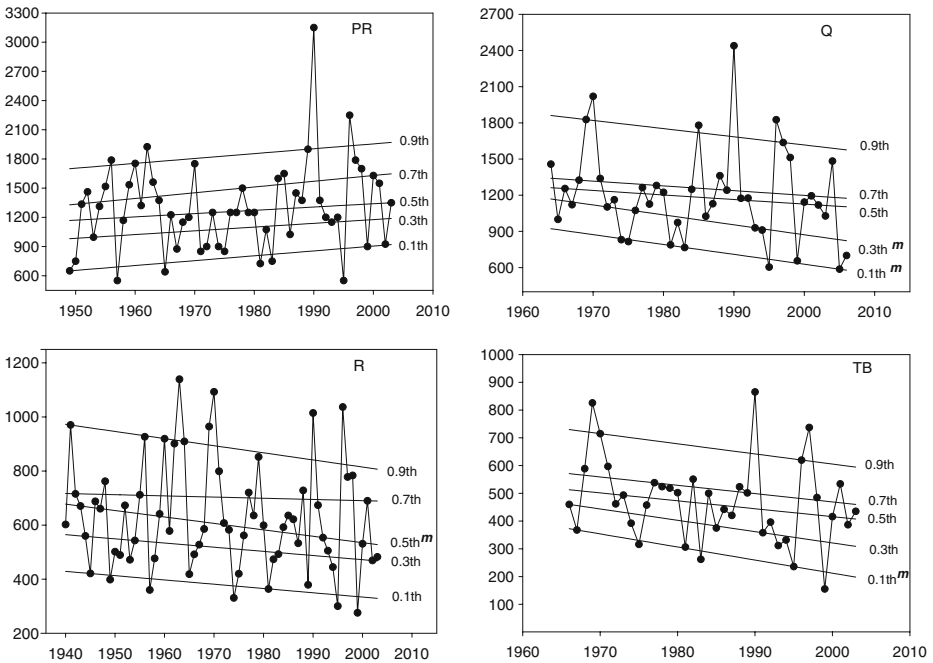


Fig. 2 (continued)

(Fig. 2). During the study period, there was no evidence of changes in higher parts of the rainfall distribution (except for GR).

3.2 Radial growth and carbon isotope discrimination

The mean age (at dbh) of the studied trees was 60 ± 5 years (mean \pm standard error) and 54 ± 5 years for firs and pines, respectively. The BAI of *A. pinsapo* increased toward the end of the 1960s and remained at about 6.7 cm^2 until the onset of the 1990s, after which time it began decreasing (Fig. 3a). From 1970 onwards, minimum values were recorded in 1995, 1998, 1999 and 2005. BAI values for *P. halepensis* also markedly increased toward the end of the 1960s but remained at about 18.3 cm^2 until 2005. The mean value during the 1990–2005 period was 4.5 cm^2 for *A. pinsapo* and 22.2 cm^2 for *P. halepensis* (Fig. 3). As for *A. pinsapo*, 1995, 1999 and 2005 showed below-average BAI values for *P. halepensis* (Fig. 3b, bottom), but the lowest values for this species were recorded in 1971 and 1982.

$\delta^{13}\text{C}$ was higher for *P. halepensis* (mean of -24.91‰ versus -26.17‰ for *A. pinsapo*, Fig. 4a), and it did not show significant trends over the second half of the twentieth century (Table 2). In contrast, *A. pinsapo* $\delta^{13}\text{C}$ decreased about -0.15‰ per decade over the same period. Δ decreased by about -0.23‰ per decade for *P. halepensis* but only decreased by -0.10‰ per decade for *A. pinsapo*. Both decreasing slopes were significantly different under the two-slope comparison test (Table 2). The mean Δ values for 1990–2005 were significantly lower (17.5‰ versus

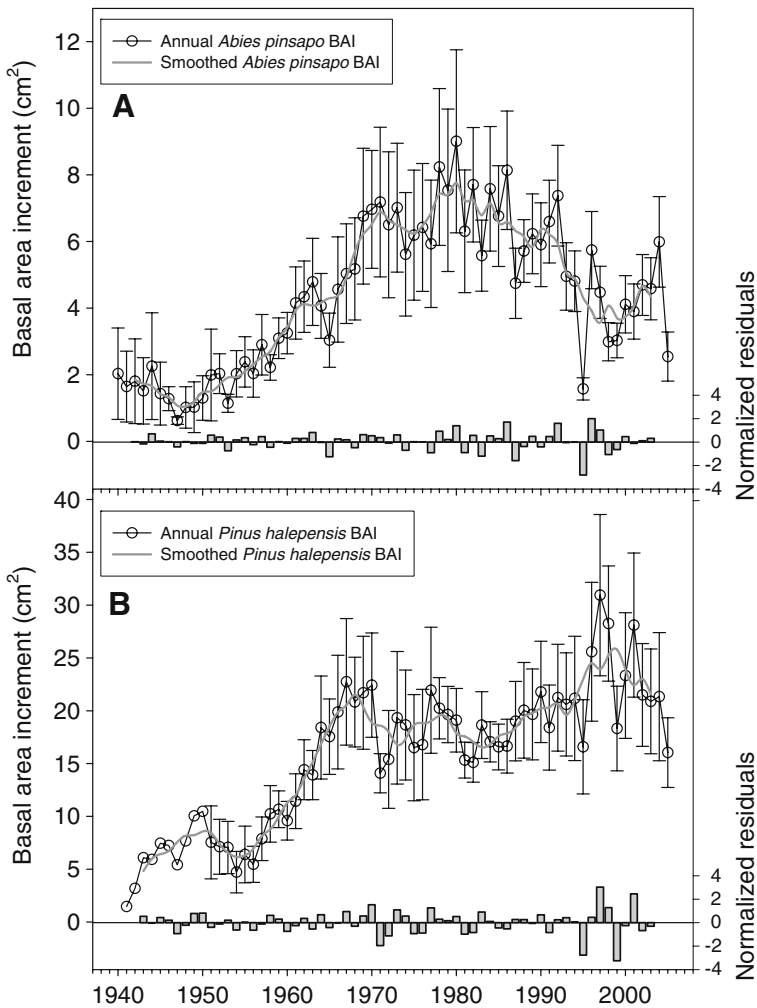


Fig. 3 Variations in basal area increment (BAI) for *Abies pinsapo* (a) and *Pinus halepensis* (b). Points represent the mean values, error bars represent the standard error, the gray line represents the moving average BAI using a 5-year window, and the bottom bars represent the normalized residuals between the values and the moving average differences

18.7%, from repeated measures ANOVA) for pine trees. We also found significant differences between both the mean values and the slopes of WUE_i of the two species over the study period (Fig. 4c). For the last 10 years (1995–2005), the mean value was $85.48 \pm 0.97 \mu\text{mol mol}^{-1}$ for *A. pinsapo*, while *P. halepensis* showed significantly higher values ($96.89 \pm 1.06 \mu\text{mol mol}^{-1}$). Although the mean values between 1950 and 1960 were about $70 \mu\text{mol mol}^{-1}$ for both species, after 1970, the mean WUE_i increased by $0.43 \mu\text{mol mol}^{-1}$ per year for *A. pinsapo* and $0.51 \mu\text{mol mol}^{-1}$ per year for *P. halepensis* (Fig. 4c; Table 2).

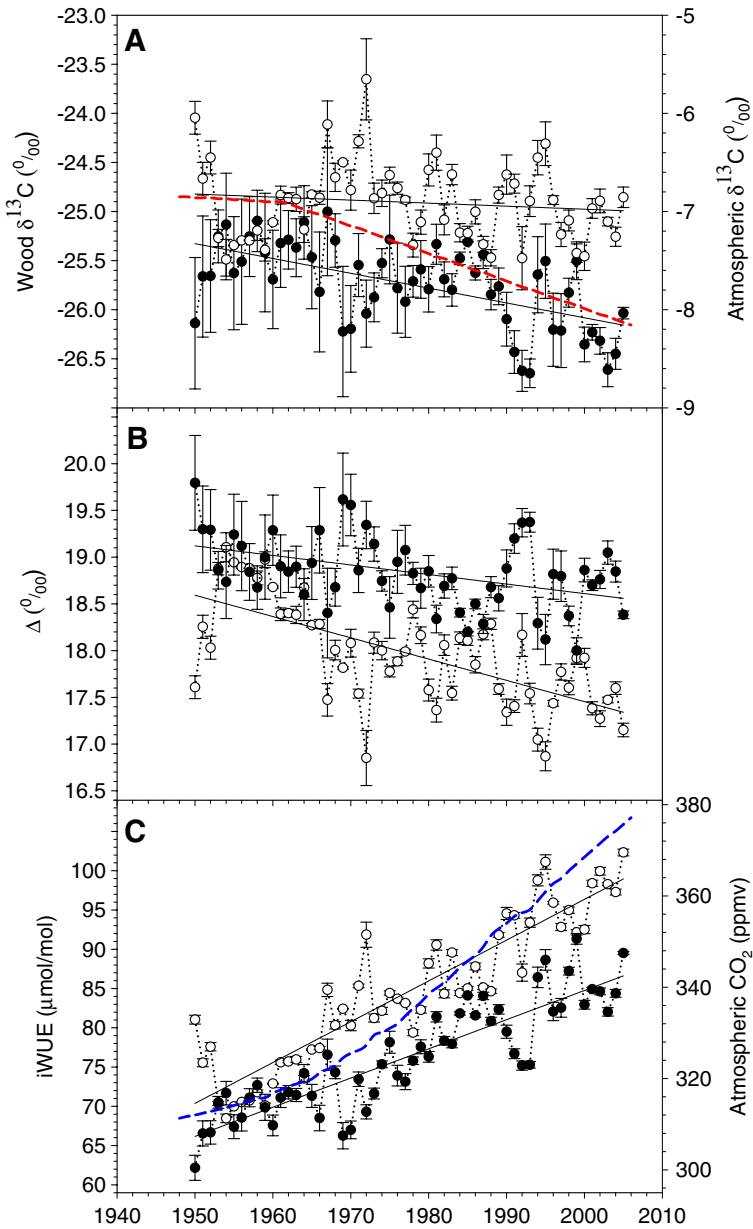


Fig. 4 Variations in wood carbon isotope signal (wood $\delta^{13}\text{C}$, **a**), plant carbon isotope discrimination (Δ , **b**) and intrinsic water use efficiency (WUE_i, **c**) for *Abies pinsapo* (black points) and *Pinus halepensis* (white points). Points represent the mean values; error bars represent the standard error. The linear regression parameters are shown in Table 2. The dashed lines show global atmospheric $\delta^{13}\text{C}$ (**a**) and CO_2 (**c**) from McCarroll and Loader (2004)

Table 2 Trends in wood ^{13}C , Δ and WUEi for *A. pinsapo* and *P. halepensis* spanning the second half of the twentieth century (1950–2006)

	Parameter	α	β	Residual SD	R^2 (adj)
<i>Abies pinsapo</i>	$\delta^{13}\text{C}_{\text{wood}}$	4.12 (5.67)	-0.015 (0.0029)a	0.35	0.34**
<i>Pinus halepensis</i>		-18.80	-0.003 (0.0033)b	0.40	0.02 ns
<i>Abies pinsapo</i>	Δ	39.04 (5.73)	-0.010(0.0029)a	0.35	0.19**
<i>Pinus halepensis</i>		62.99 (6.75)	-0.023 (0.0034)b	0.41	0.44**
<i>Abies pinsapo</i>	WUEi	-658.66	0.37 (0.027)a	3.30	0.77**
<i>Pinus halepensis</i>		-943.10	0.52 (0.031)b	3.80	0.83**

Standard deviation is shown in brackets. Different letters denote significant differences between slopes (two-slope comparison test, $n = 56$)

α the intercept, β the slope, *ns* not significant

** $p < 0.01$

3.3 Climate relationships

Correlations between BAI and Δ , and the local average climate (obtained by mean monthly temperature and precipitation from Q, B and AZ stations, see Table 1) appear in the Table 3. For *P. halepensis*, values of standardized BAI were positively correlated with January, March and current September temperatures and previous autumn to winter precipitations, while previous November and May temperatures yielded a negative correlation. *A. pinsapo* standardized BAI was positively related to previous late autumn to early winter temperatures, and May and September precipitations; July precipitation yielded a negative effect likely because it was inversely correlated to June and July temperatures (-0.36 and -0.27 respectively). We found a negative correlation between *P. halepensis* wood Δ and March and June temperatures, while September temperature correlation was positive. February and June precipitation were positively correlated but March and August precipitation were negatively correlated to *P. halepensis* wood Δ (Table 3). *A. pinsapo* wood Δ was negatively correlated to October and November temperatures. Previous autumn to early spring, June and October precipitations were positively correlated but July and august precipitations were negatively correlated with *A. pinsapo* wood Δ .

Correlations patterns obtained from the regional average climate appear in the Table 4. For *P. halepensis*, the negative correlation between standardized BAI and May temperature disappeared but previous October and August yielded now significant correlations. *A. pinsapo* standardized BAI was only positively correlated to previous December temperature, while May and June temperature yielded now significant negative correlations. Correlations patterns between standardized BAI and precipitation were quite similar to these showed for the local scale analysis, however only four of the nine significant correlations found between *A. pinsapo* wood Δ and precipitations, using the local climate series, were retained for the regional one.

The WUEi values for both species were strongly correlated with global atmospheric CO_2 (Spearman $r = 0.89$; $p < 0.001$ for *A. pinsapo* and $r = 0.92$; $p < 0.001$ for *P. halepensis*). The mean increase in WUEi for *A. pinsapo* was about $0.298 \mu\text{mol mol}^{-1} \text{ppmv}^{-1}$ of atmospheric CO_2 increase. For *P. halepensis*, this change was about $0.417 \mu\text{mol mol}^{-1} \text{ppmv}^{-1}$. Finally, the BAI was positively correlated with Δ for *A. pinsapo* (Spearman $r = 0.27$; $p = 0.04$), but not for *P. halepensis* (Spearman $r = 0.02$; $p = 0.91$).

Table 3 Spearman correlation coefficients obtained for the normalized residuals of BAI (left) and Δ (right) with local monthly temperature and precipitation obtained from the three closest stations to the sampling area (Q, B and AZ, see Table 1). **: $p < 0.01$; *: $p < 0.05$

Month	Basal area increment (BAI)						Carbon isotope ratio (Δ)					
	Temperature		Precipitation		Temperature		Precipitation		Temperature		Precipitation	
	<i>P. halepensis</i> <i>r</i> Spearman	<i>A. pinsapo</i> <i>r</i> Spearman	<i>P. halepensis</i> <i>r</i> Spearman	<i>A. pinsapo</i> <i>r</i> Spearman	<i>P. halepensis</i> <i>r</i> Spearman	<i>A. pinsapo</i> <i>r</i> Spearman	<i>P. halepensis</i> <i>r</i> Spearman	<i>A. pinsapo</i> <i>r</i> Spearman	<i>P. halepensis</i> <i>r</i> Spearman	<i>A. pinsapo</i> <i>r</i> Spearman	<i>P. halepensis</i> <i>r</i> Spearman	<i>A. pinsapo</i> <i>r</i> Spearman
September -1	-0.14	-0.03	0.15*	-0.01	0.15	-0.16	0.00	0.21*	0.04	0.00	0.21*	0.21*
October -1	-0.07	0.11*	0.22**	-0.01	0.13	-0.01	-0.08	0.29**	0.15	-0.08	0.29**	0.29**
November -1	- 0.16*	0.12*	0.25**	0.03	0.07	-0.12	0.08	0.06	0.15	0.08	-0.06	-0.06
December -1	0.13	0.13*	0.24**	0.16*	0.11	-0.07	0.14	0.24*	0.03	0.14	0.24*	0.24*
January	0.20**	0.00	0.22**	0.21**	-0.06	-0.10	0.06	0.23*	-0.06	0.06	0.23*	0.23*
February	0.11	0.06	-0.07	0.12	0.01	-0.09	0.23*	0.04	0.01	0.23*	0.04	0.04
March	0.18**	- 0.16*	-0.08	0.14	- 0.18*	-0.09	- 0.17*	0.31**	- 0.18*	- 0.17*	0.31**	0.31**
April	0.06	-0.11	-0.06	0.06	-0.01	-0.07	0.12	0.15	-0.01	0.12	0.15	0.15
May	- 0.17*	-0.12	0.07	0.29**	-0.12	-0.06	0.15	0.03	-0.12	0.15	0.03	0.03
June	-0.09	-0.09	0.13*	0.04	- 0.18*	-0.02	0.23*	0.20*	- 0.18*	0.23*	0.20*	0.20*
July	-0.10	0.00	-0.07	- 0.20*	0.06	-0.08	0.06	- 0.28**	0.06	0.06	- 0.28**	- 0.28**
August	0.00	-0.05	0.04	-0.06	0.07	-0.01	- 0.19*	0.15	0.07	- 0.19*	0.15	- 0.19*
September	0.17*	-0.02	0.01	0.16*	0.39**	-0.04	-0.07	0.06	- 0.19*	-0.07	0.06	0.15
October	0.00	-0.04	-0.10	0.10	0.10	- 0.21*	-0.13	0.32**	0.10	-0.13	0.32**	0.32**
November	0.06	-0.05	0.03	0.05	-0.08	- 0.21*	0.06	0.07	-0.08	0.06	0.07	0.07
December	-0.06	-0.03	-0.08	-0.04	0.11	-0.15	-0.07	-0.07	0.11	-0.07	-0.07	-0.07

** $p < 0.01$, * $p < 0.05$, significant results

Table 4 Spearman correlation coefficients obtained for the normalized residuals of BAI (left) and Δ (right) with regional monthly temperature and precipitation obtained from the remaining nine stations (see Table 1). **: $p < 0.01$; *: $p < 0.05$

Month	Basal area increment (BAI)						Carbon isotope ratio (Δ)					
	Temperature			Precipitation			Temperature			Precipitation		
	<i>P. halepensis</i> <i>r</i> Spearman	<i>A. pinsapo</i> <i>r</i> Spearman	<i>A. pinsapo</i> <i>r</i> Spearman	<i>P. halepensis</i> <i>r</i> Spearman	<i>P. halepensis</i> <i>r</i> Spearman	<i>A. pinsapo</i> <i>r</i> Spearman	<i>P. halepensis</i> <i>r</i> Spearman	<i>P. halepensis</i> <i>r</i> Spearman	<i>A. pinsapo</i> <i>r</i> Spearman	<i>P. halepensis</i> <i>r</i> Spearman	<i>P. halepensis</i> <i>r</i> Spearman	<i>A. pinsapo</i> <i>r</i> Spearman
September -1	-0.11	-0.05	0.10	0.20**	0.10	0.10	0.10	-0.03	-0.12	-0.03	0.18*	
October -1	-0.13*	0.02	0.04	0.18**	0.10	0.04	0.10	0.09	-0.01	0.09	0.12	
November -1	-0.12*	-0.03	0.04	0.13	0.12	0.04	0.12	0.03	-0.10	0.03	-0.13	
December -1	0.09	0.13**	0.12**	0.18**	0.13	0.12**	0.13	0.22**	-0.06	0.22**	0.12	
January	0.19**	0.00	0.14**	0.18**	-0.09	0.14**	-0.09	0.03	-0.06	0.03	0.14	
February	0.10	-0.06	0.09	-0.09	-0.03	0.09	-0.03	0.13	-0.12	0.13	0.03	
March	0.17**	-0.12**	0.15**	-0.10	-0.07	0.11**	-0.07	0.14	-0.08	0.14	0.31**	
April	0.11	-0.07	0.11**	-0.12	0.08	0.11**	0.08	0.05	0.06	0.05	0.05	
May	-0.05	-0.12**	0.31**	0.08	0.17	0.31**	0.17	0.04	-0.08	0.04	0.05	
June	-0.07	-0.14**	0.11	0.16**	-0.17	0.11	-0.17	0.22**	-0.07	0.22**	0.03	
July	-0.05	0.01	-0.10	-0.08	-0.22**	-0.10	-0.22**	0.14	-0.09	0.14	-0.24**	
August	0.12*	0.00	-0.03	0.02	-0.12	-0.03	-0.12	-0.05	-0.06	-0.05	-0.11	
September	0.20*	0.06	0.07	-0.07	0.23**	0.07	0.23**	-0.09	-0.14	-0.09	0.10	
October	0.02	-0.04	0.04	-0.06	-0.01	0.04	-0.01	0.10	-0.29**	0.10	0.20**	
November	0.05	-0.11	0.09	0.03	-0.06	0.09	-0.06	0.03	-0.16	0.03	0.00	
December	-0.13	-0.10	0.00	0.02	0.06	0.00	0.06	0.06	-0.18	0.06	-0.05	

** $p < 0.01$, * $p < 0.05$, significant results

4 Discussion

In recent decades, the global climate has tended towards warmer conditions (IPCC 2007), strongly affecting plant performance (Peñuelas and Filella 2001). In the study area, the mean temperature increased by an average of 1.04°C between 1920 and 2004 (0.12°C per decade), with major enhancements since 1970 (0.33°C per decade). Across Europe, the observed temperature has increased by about 0.8°C during the twentieth century (IPCC 2001). Trends in annual precipitation reflect more spatial variability (Fig. 2), although overall drying trends have prevailed. This observation agrees, for instance, with a reported decrease in the number of days with precipitation over the Spanish southern coast in 1964–1993 (Romero and Ramis 1999; Sumner et al. 2003). The P-ETP values show strong decadal-scale variability in drought frequency; the mid-1940s, mid-1970s, early 1980s and early 1990s experienced widespread and severe droughts (Fig. 1). Recently, dry conditions were again observed in 2005, suggesting an increase over the twentieth century in drought extremes.

Quantile regression analyses allow us to conclude that the lowest part of the rainfall distribution (i.e., the driest years) experienced overall negative trends. Our results indicate that, although no changes in mean rainfall were statistically detectable at most of the studied stations, the dry years became even drier during the study period (Fig. 2). Consistent with the quantile regression results, seven of the ten lowest values observed since 1920 occurred in the last 30 years, according to the annual P-ETP record. From a spatial point of view, orography and atmospheric circulation patterns lead to high mean precipitation values at the southwestern edge of the Betic range, as compared to the Iberian average. On the western side of the study Region the precipitation is mostly dominated by Atlantic fronts, while the eastern side of its domain is more under Mediterranean influence and summer storms and Mediterranean cyclogenesis are the dominant factors influencing precipitation. Most of the annual rainfall, carried by low pressure systems coming from Atlantic depressions, falls on the western part of the study area and decreases toward the eastern part (Table 1). In addition, temporal climatic trends also reveal a higher dryness at locations far from the Mediterranean coast, as has been demonstrated by Millán et al. (2005) for eastern Spain. This complex sub-regional pattern has been related to changes in the summer storm regime. Land-use perturbations that have accumulated over time and greatly accelerated over the last 30 years may have induced changes from frequent summer storms over the mountains inland to a regime dominated by closed vertical recirculation in which feedback mechanisms favor the loss of storms over the coastal mountains during the summer (Millán et al. 2005). In addition to the above discussed summer storms decrease, Atlantic frontal precipitation could be also decreasing in the region, while Mediterranean cyclogenesis is not only increasing, but becoming more torrential in nature. As a consequence of this, the period of water availability for the trees in the area would be changing, with less precipitation in spring and summer and more precipitation of a more torrential nature in autumn (Millán et al. 2005).

BAI and wood Δ were positively related to precipitation in *A. pinsapo* and *P. halepensis*, reflecting the effect of water availability on biomass gain and the water-carbon balance of both species. Previous autumn, winter and June precipitations were positively correlated to *P. halepensis* BAI, while previous December to May

did for *A. pinsapo*. Several authors have mainly reported relationships between indicators of water availability and wood Δ in conifers (Korol et al. 1999; Warren et al. 2001); however, Δ was also significantly related to temperature, as in previous studies that placed temperature among the factors best correlated with Δ (Anderson et al. 1998; Brooks et al. 1998). Negative correlations for March and June temperature reflect water use efficiency increase, likely interacting with common reduced water availability on this period. By opposite, *P. halepensis* Δ and BAI showed positive correlations with September temperature, which could be reflecting growth enhancement during the autumn latewood formation, when water stress again diminishes.

The weak relationships between Δ and temperature conditions for *A. pinsapo* may indicate carbon uptake and secondary growth occurs in the fir mainly as a function of water availability. In this sense, precipitation was widely related to Δ and BAI for *A. pinsapo* throughout the year (Tables 3 and 4). This result suggests that *A. pinsapo* relies primarily on precipitation amounts at the onset or throughout the growing period and, to a lesser extent, on groundwater, which agrees with other dendroecological studies of this species (Linares et al. 2009b). Furthermore, July and August precipitation showed negative correlation with Δ , which could be likely related to a moisture-induced growth enhancement during the warmer period; the same relationship was yielded for *P. halepensis* wood Δ and August precipitation.

Despite global increases in atmospheric CO₂ since the 1980s, the rate of WUEi increase in *A. pinsapo* has been halted, no longer following the CO₂ trend (Linares et al. 2009c). Although the reason for this decoupling is not well understood, our data support an agreement between the starting points of the WUEi slope decrease (~1980; Fig. 3c) and the regional dryness, which also suggests a water limitation-induced prevention of WUEi increase, as reported by Peñuelas et al. (2008). The recent reduction in the WUEi response to increasing CO₂ in water-limited trees may be related to a loss in adaptation capacity derived from a low drought avoidance threshold (Linares et al. 2009c). This may have resulted in reduced transpiration and decreasing biomass gains, as reflected in the low BAI for *A. pinsapo* throughout the second half of the XX century (Linares et al. 2009a).

The growth for *P. halepensis* trees was strongly related to temperature (Table 3), which could be explained by the fact that, at the study site, the annual precipitation is higher and the mean temperature is lower than the average for the Aleppo pine range. The lack of a relationship between spring precipitation and radial growth for *P. halepensis* has also been observed in other conifers (Lebourgeois 2000) and can be explained by spring radial growth being partly supported by previous-year photosynthates and moisture reserves supplied by precipitation prior to growth (Table 3). In addition, recent findings showed that *P. halepensis* growth can be sustained by deeper moisture reserves supplied by precipitation delivered even several months prior to growth (Sarris et al. 2007). On the other hand, the wood Δ of *P. halepensis* was related to the summer rainfall, which contrasts with the previously reported nearly constant relationship between Δ and precipitation throughout the year, as we obtained for *A. pinsapo* wood Δ , in agreement with the short-term rainfall dependence of Mediterranean conifers (Nicault et al. 2001; Ferrio and Voltas 2005). This discrepancy can be explained by the fact that the studied *P. halepensis* population is located at one of the moister locations for this species (1,100 mm year⁻¹ on average), and therefore, precipitation only exert an important control on Δ during

the summer, when water availability is the main limiting factor for photosynthesis (Ferrio et al. 2003).

The observed increase in mean temperature and decrease in water budget (Fig. 1) may reflect a depletion of water resources in the early spring at the onset of the growing season, resulting in the reduced secondary growth of *A. pinsapo* (Linares et al. 2009b). Conversely, *P. halepensis* is considered to be a very flexible species, showing two periods of climate-driven cambial activity: one defined by the summer drought and the other by low winter temperatures (Liphshitz and Lev-Yadun 1986). In this sense, the positive association between January temperature and BAI suggests that pine growth is also limited to some extent by cold temperatures in the winter (Tables 3 and 4). Vila et al. (2008) also studied growth trends at *P. halepensis* upper altitudinal/northern latitudinal range (south-eastern Mediterranean France, Sainte-Baume Mountain area) and reported constantly increasing wood productivity towards the end of the twentieth century. The growth improvement in *P. halepensis* was mainly attributed to the recorded increase in minimum temperatures similar to the findings reported here. Vennetier and Hervé (1999) also evidenced a recent increase in height growth for the species in south-eastern France. Therefore, an increase in the length of the growing season, during which milder temperatures occur, might cause increased secondary growth in Aleppo pine trees, while further decline and replacement of *A. pinsapo* would be expected due to more prevalent drought conditions (Linares et al. 2009c).

Our results support the hypothesis that species with higher drought sensitivity would show more sudden reductions in growth under drier conditions, as compared to better drought-adapted species, even with shared drought-avoiding strategies (Martínez-Vilalta and Piñol 2002). The ecophysiology of *A. pinsapo* is currently poorly understood (but see Aussenac 2002). This endangered tree drastically reduces water loss in response to moderate drought conditions and shows a pre-formed growth pattern (Linares et al. 2009b). Decline symptoms based on growth trends similar to those of *A. pinsapo* have already been identified near the southern edge of the distribution of *A. alba*, in agreement with the decreasing numbers of days with precipitation over the Pyrenees (Romero and Ramis 1999; Macias et al. 2006).

If, as climate change models predict, the frequency of drought events in the Mediterranean basin increases as a result of rising temperatures and decreasing spring precipitation (Sumner et al. 2001), we may witness further declines in tree growth, since spring precipitation was found to be critical for *A. pinsapo* growth (Tables 3 and 4). Long-term decreases in *A. pinsapo* secondary growth caused by regional warming and water shortages suggest that warming temperatures and changing precipitation patterns increase drought stress on this species. Moreover, *A. pinsapo* will likely display lower radial growths in climates with predicted increased seasonal variability, regardless of the total amount of precipitation, since this relict fir still preserves several physiological features from its Arcto-Tertiary origin that are, to some extent, out of phase with the requirements of a spring-to-summer drought-increasing habitat (Aussenac 2002). In contrast, *P. halepensis* is well adapted to the scarcity of water resources (Borghetti et al. 1998), and the sustained free growth pattern of this species allows it to cease growth during drought events and to recover it rapidly when water becomes available (Rathgeber et al. 2005; Nicault et al. 2001). Finally, increased water-use efficiency does not prevent the warming-induced growth decline of *A. pinsapo*. *P. halepensis*, on the other hand, showed slight increases in

BAI and WUEi over the last 30 years, indicating that pine trees are able to maintain constant secondary growth and lower water costs under increasing water stress.

5 Conclusions

We report changing climatic conditions, drought-induced limitations of radial growth and a decreasing improvement of WUEi for *A. pinsapo*. Our results allow us to conclude that both *A. pinsapo* and *P. halepensis* respond to a decrease in water availability by increasing their WUEi, as inferred from wood Δ . However, *A. pinsapo* growth is more sensitive to spring water availability, showing a steeper decline in BAI with increasing dryness. This is in agreement with the hypothesis that species with higher drought sensitivity would show smaller increases in WUEi and sudden growth reductions under drier conditions than species with better adaptations to drought, even if they share drought-avoiding strategies.

Acknowledgements The authors are grateful to Dr. J.J. Camarero for dendroecological lessons. This study was supported by “Junta de Andalucía” projects CVI-302 and RNM-296. JCL acknowledges a MEC-FPU grant. We thank S.H. Schneider, K. Kivel, B.S. Cade and two anonymous reviewers for improve a previous version of this paper.

References

- Adams HD, Guardiola-Claramonte M, Barron-Gafford GA et al (2009) Temperature sensitivity of drought-induced tree mortality: implications for regional die-off under global-change-type drought. *PNAS* 106:7066–7063
- Allen CD, Macalady AK, Chenchouni H et al (2010) A global overview of drought and heat-induced tree mortality reveals emerging climate change risks for forests. *For Ecol Manag* 259:660–684
- Anderson WT, Bernasconi SM, McKenzie JA, Saurer M (1998) Oxygen and carbon isotopic record of climatic variability in tree ring cellulose (*Picea abies*): an example from central Switzerland (1913–1995). *J Geophys Res* 103:625–636
- Andreu L, Gutiérrez E, Macias M, Ribas M, Bosch O, Camarero JJ (2007) Climate increases regional tree-growth variability in Iberian pine forests. *Glob Chang Biol* 13:1–12
- Aussenac G (2002) Ecology and ecophysiology of circum-Mediterranean firs in the context of climate change. *Ann For Sci* 59:823–832
- Borghetti M, Cinnirella S, Magnani F, Saracino A (1998) Impact of long term drought on xylem embolism and growth in *Pinus halepensis* Mill. *Trees Struct Funct* 12:187–195
- Brooks JR, Flanagan LB, Ehleringer JR (1998) Responses of boreal conifers to climate fluctuations: indications from tree-ring widths and carbon isotope analyses. *Can J For Res* 28:524–533
- Brubaker LB (1986) Responses of tree populations to climatic change. *Plant Ecol* 67:119–130
- Brunet M, Sigro J, Saladie O et al (2005) Long-term change in the mean and extreme state of surface air temperature over Spain (1850–2003). *Geophys Res Abstr* 7
- Brunetti M, Buffoni L, Mangianti F, Maugeri M, Nanni T (2004) Temperature, precipitation and extreme events during the last century in Italy. *Glob Planet Change* 40:141–149
- Cade BS, Noon BR (2003) A gentle introduction to quantile regression for ecologists. *Front Ecol Environ* 1:412–420
- Chbouki N, Stockton CW, Myers DE (1995) Spatio-temporal patterns of drought in Morocco. *Int J Climatol* 15:187–205
- Esteban-Parra MJ, Rodrigo FS, Castro-Diez Y (1998) Spatial and temporal patterns of precipitation in Spain for the period 1880–1992. *Int J Climatol* 18:1557–1574
- Farquhar GD, Richards RA (1984) Isotopic composition of plant carbon correlates with water-use efficiency of wheat genotypes. *Aust J Plant Physiol* 11:539–552

- Farquhar GD, O'Leary HM, Berry JA (1982) On the relationship between carbon isotope discrimination and the intercellular carbon dioxide concentration in leaves. *Aust J Plant Physiol* 9:121–137
- Feidas H, Nouloupoulou N, Makrogiannis T, Bora-Senta E (2007) Trend analysis of precipitation time series in Greece and their relationship with circulation using surface and satellite data: 1955–2001. *Theor Appl Climatol* 87:155–177
- Ferrio JP, Voltas J (2005) Carbon and oxygen isotope ratios in wood constituents of *Pinus halepensis* as indicators of precipitation, temperature and vapour pressure deficit. *Tellus, Ser B Chem Phys Meteorol* 164–173
- Ferrio JP, Florit A, Vega A, Serrano L, Voltas J (2003) $\Delta^{13}\text{C}$ and tree-ring width reflect different drought responses in *Quercus ilex* and *Pinus halepensis*. *Oecologia* 137:512–518
- Fritts HC (1976) *Tree rings and climate*. Academic, London
- García JA, Gallego MC, Serrano A, Vaquero JM (2007) Trends in block-seasonal extreme rainfall over the Iberian Peninsula in the second half of the twentieth century. *J Climate* 20:113–130
- Giorgi F (2002) Variability and trends of sub-continental scale surface climate in the twentieth century. Part I: observations. *Clim Dyn* 18:675–791
- González-Hidalgo JC, De Luis M, Raventós J, Sánchez JR (2001) Spatial distribution of seasonal rainfall trends in a western Mediterranean area. *Int J Climatol* 21:843–860
- Goodess CM, Jones PD (2002) Links between circulation and changes in the characteristics of Iberian rainfall. *Int J Climatol* 22:1593–1615
- Heaton THE (1999) Spatial, species, and temporal variations in the $^{13}\text{C}/^{12}\text{C}$ ratios of C_3 plants: implications for palaeodiet studies. *J Archaeol Sci* 26:637–649
- Holmes RL (1983) Computer-assisted quality control in tree-ring dating and measurement. *Tree-Ring Bull* 43:68–78
- Holmes RL (1992) *Dendrochronology program library*. Laboratory of Tree-Ring Research, University of Arizona, Tucson
- IPCC (2001) *Climate change 2001: impacts, adaptation and vulnerability*. In: McCarthy JJ, Canziani OF, Leary NA (eds) *Contribution of working groups II to the third assessment report of the intergovernmental panel on climate change*. Cambridge University Press, Cambridge
- IPCC (2007) *Climate change, fourth assessment report*. Cambridge University Press, London
- Kendall MG (1975) *Rank correlation methods*. Charles Griffin, London
- Klein Tank AMG et al (2002) Daily dataset of 20th century surface air temperature and precipitation series for the European climate assessment. *Int J Climatol* 22:1441–1453
- Koenker R (2005) *Quantile regression*. Cambridge University Press, Cambridge
- Korol RL, Kirschbaum MUF, Farquhar GD, Jeffreys M (1999) Effects of water status and soil fertility on the C-isotope signature in *Pinus radiata*. *Tree Physiol* 19:551–562
- Lana X, Martínez MD, Burgueño A, Serra C, Martín-Vide J, Gómez L (2008) Spatial and temporal patterns of dry spell lengths in the Iberian Peninsula for the second half of the twentieth century. *Theor Appl Climatol* 91:99–116
- Lebourgeois F (2000) Climatic signals in earlywood, latewood and total ring width of Corsican pine from western France. *Ann For Sci* 57:155–164
- Libiseller C, Grimvall A (2002) Performance of partial Mann Kendall tests for trend detection in the presence of covariates. *Environmetrics* 13:71–84
- Linares JC, Carreira JA (2009) Temperate-like stand dynamics in relict Mediterranean-fir (*Abies pinsapo*, Boiss.) forests from Southern Spain. *Ann For Sci* 66:610–620
- Linares JC, Camarero JJ, Carreira JA (2009a) Interacting effects of climate and forest-cover changes on mortality and growth of the southernmost European fir forests. *Glob Ecol Biogeogr* 18:485–497
- Linares JC, Camarero JJ, Carreira JA (2009b) Plastic responses of *Abies pinsapo* xylogenesis to drought and competition. *Tree Physiol* 29:1525–1536
- Linares JC, Delgado-Huertas A, Camarero JJ, Merino J, Carreira JA (2009c) Competition and drought limit the water-use efficiency response to rising atmospheric CO_2 in the Mediterranean fir *Abies pinsapo*. *Oecologia* 161:611–624
- Linares JC, Camarero JJ, Carreira JA (2010) Competition modulates the adaptation capacity of forests to climatic stress: insights from recent growth decline and death in relict stands of the Mediterranean fir *Abies pinsapo*. *J Ecol* 98:592–603
- Lindner M, Maroschek M, Netherer S et al (2010) Climate change impacts, adaptive capacity, and vulnerability of European forest ecosystems. *For Ecol Manag* 259:698–709
- Liphshitz N, Lev-Yadun S (1986) Cambial activity of evergreen and seasonal dimorphics around the Mediterranean. *IAWA Bull* 7:145–153

- Macias M, Andreu L, Bosch O, Camarero JJ, Gutiérrez E (2006) Increasing aridity is enhancing silver fir *Abies alba* (Mill.) water stress in its south-western distribution limit. *Clim Change* 79:289–313
- Maheras P, Anagnostopoulou C (2003) Circulation types and their influence on the interannual variability and precipitation changes in Greece. In: Bolle HJ (ed) *Mediterranean climate variability and trends*. Springer, Berlin, pp 215–239
- Mann HB (1945) Nonparametric tests against trend. *Econometrica* 13:245–259
- Martínez-Vilalta J, Piñol J (2002) Drought-induced mortality and hydraulic architecture in pine populations of the NE Iberian Peninsula. *For Ecol Manag* 161:247–256
- Martínez-Vilalta J, López BC, Adell N, Badiella L, Ninyerola M (2008) Twentieth century increase of Scots pine radial growth in NE Spain shows strong climate interactions. *Glob Chang Biol* 14:2868–2881
- McCarroll D, Loader NJ (2004) Stable isotopes in tree-rings. *Quat Sci Rev* 23:771–801
- McDowell N, Allen CD, Marshall L (2010) Growth, carbon isotope discrimination, and climate-induced mortality across a *Pinus ponderosa* elevation transect. *Glob Chang Biol* 16:399–415
- McNulty SG, Swank WT (1995) Wood 13C as a measure of annual basal area growth and soil water stress in a *Pinus strobus* forest. *Ecology* 76:1581–1586
- Médail F, Quézel P (1999) Biodiversity hotspots in the Mediterranean basin: setting global conservation priorities. *Conserv Biol* 13:1510–1513
- Millán MM, Estrela MJ, Sanz MJ et al (2005) Climatic feedbacks and desertification: the Mediterranean model. *J Climate* 18:684–701
- Nicault A, Rathgeber C, Tessier L, Thomas A (2001) Observations on the development of rings of Aleppo pine (*Pinus halepensis* Mill.): confrontation between radial growth, density and climatic factors. *Ann For Sci* 58:769–784
- Norrant C, Douguédroit A (2006) Monthly and daily precipitation trends in the Mediterranean (1950–2000). *Theor Appl Climatol* 88:89–106
- O'Leary MH (1981) Carbon isotope fractionation in plants. *Phytochemistry* 20:553–567
- Osmond CB, Björkman O, Anderson DJ (1980) *Physiological processes in plant ecology*. Springer, New York
- Peñuelas J, Filella I (2001) Phenology: responses to a warming world. *Science* 294:793–795
- Peñuelas J, Hunt JM, Ogaya R, Alistair SJ (2008) Twentieth century changes of tree-ring d13C at the southern range-edge of *Fagus sylvatic*: increasing water-use efficiency does not avoid the growth decline induced by warming at low altitude. *Glob Chang Biol* 14:1–13
- Piervitali E, Colacino M, Conte M (1997) Signals of climatic change in the Central-Western Mediterranean Basin. *Theor Appl Climatol* 58:211–219
- R Development Core Team (2010) R: a language and environment for statistical computing. R Foundation for Statistical Computing, Vienna, Austria. ISBN 3-900051-07-0. Available at <http://www.R-project.org>.
- Räsänen J, Hansson U, Ullerstig A et al (2004) European climate in the late twenty-first century: regional simulations with two driving global models and two forcing scenarios. *Clim Dyn* 22:13–31
- Rathgeber BK, Misson L, Nicault A, Guiot J (2005) Bioclimatic model of tree radial growth: application to the French Mediterranean Aleppo pine forests. *Trees Struct Funct* 19:162–176
- Romero R, Ramis C (1999) Daily rainfall patterns in the Spanish Mediterranean area: an objective classification. *Int J Climatol* 19:95–112
- Sarris D, Christodoulakis D, Körner C (2007) Recent decline in precipitation and tree growth in the eastern Mediterranean. *Glob Chang Biol* 13:1–14
- Schweingruber FH (1988) *Tree rings. Basics and applications of dendrochronology*. Dordrecht, Boston
- Serra C, Burgueño A, Martínez MD, Lana X (2005) Trends of dry spells across Catalonia (NE Spain) for the second half of the 20th century. *Theor Appl Climatol* 85:165–183
- Sumner G, Homar V, Ramis C (2001) Precipitation seasonality in eastern and southern coastal Spain. *Int J Climatol* 21:219–247
- Sumner G, Romero R, Homar V, Ramis C, Alonso S, Zorita E (2003) An estimate of the effects of climate change on the rainfall of Mediterranean Spain by the late twenty first century. *Clim Dyn* 20:789–805
- Taylor AM, Brooks JR, Lachenbruch B, Morrell JJ, Voelker S (2008) Correlation of carbon isotope ratios in the cellulose and wood extractives of Douglas-fir. *Dendrochronologia* 26:125–131

- Touchan R, Xoplaki E, Funkhouser G et al (2005) Reconstructions of spring/summer precipitation for the Eastern Mediterranean from tree-ring widths and its connection to large-scale atmospheric circulation. *Clim Dyn* 25:75–98
- Trigo RM, Palutikof JP (2001) Precipitation scenarios over Iberia: a comparison between direct GCM output and different downscaling techniques. *J Climate* 14:4422–4446
- Türkes M, Erlat E (2003) Precipitation changes and variability in Turkey linked to the North Atlantic oscillation during the period 1930–2000. *Int J Climatol* 23:1771–1796
- Vennetier M, Hervé J (1999) Short and long term evolution of *Pinus halepensis* (Mill.) height growth in Provence, and its consequences for timber production. In: Karjaleinen T, Spiecker H, Laroussine O (eds) Tree growth acceleration in Europe. Nancy, pp 263–265
- Vicente-Serrano SM, Quadat-Prats JM (2007) Trends in drought intensity and variability in the middle Ebro valley (NE of the Iberian peninsula) during the second half of the twentieth century. *Theor Appl Climatol* 88:247–258
- Vicente-Serrano SM, Gonzalez-Hidalgo JC, De Luis M, Raventós J (2004) Drought patterns in the Mediterranean area: the Valencia region (eastern Spain). *Clim Res* 26:5–15
- Vila B, Vennetier M, Ripert C, Chandieux O, Liang E, Guibal F, Torre F (2008) Has global change induced divergent trends in radial growth of *Pinus sylvestris* and *Pinus halepensis* at their bioclimatic limit? The example of the Sainte-Baume forest (south-east France). *Ann For Sci* 65:709
- Warren CR, McGrath JF, Adams MA (2001) Water availability and carbon isotope discrimination in conifers. *Oecologia* 127:467–486
- Willmott CJ, Rowe CM, Mintz Y (1985) Climatology of the terrestrial seasonal water cycle. *Int J Climatol* 5:589–606
- Xoplaki E, González-Rouco JF, Luterbacher J, Wanner H (2004) Wet season Mediterranean precipitation variability: influence of large-scale dynamics and trends. *Clim Dyn* 23:63–78
- Zar JH (1999) Biostatistical analysis. Prentice Hall, Upper Saddle River